CP violation and matter effect in long-baseline neutrino oscillations in the four-neutrino model

Toshihiko Hattori*
Institute of Theoretical Physics, University of Tokushima, Tokushima 770-8502, Japan

Tsutom Hasuike†
Department of Physics, Anan College of Technology, Anan 774-0017, Japan

Seiichi Wakaizumi‡
School of Medical Sciences, University of Tokushima, Tokushima 770-8509, Japan
(Received 12 September 2001; published 1 April 2002)

We investigate the *CP* violation effect and the matter effect in the long-baseline neutrino oscillations in the four-neutrino model with the mass scheme of the two pairs of two close masses separated by a gap of the order of 1 eV by using the constraints on the mixing matrix derived from the solar neutrino deficit, atmospheric neutrino anomaly, LSND experiments, and the other terrestrial neutrino oscillation experiments. We also use the results of the combined analyses by Gonzalez-Garcia, Maltoni, and Peña-Garay of the solutions to the solar and atmospheric neutrino problems with the recent SNO solar neutrino data. For the solution of close-to-active solar neutrino oscillations plus close-to-sterile atmospheric neutrino oscillations, the pure *CP* violation part of the oscillation probability difference between the *CP*-conjugate channels could get as large as 0.10–0.25 in the neutrino energy range of $E=6-15$ GeV at the baseline $L=730$ km for $\nu_\mu \to \nu_\tau$ oscillation and the matter effect is at the 8–15 % level of the pure *CP* violation effect, while for the solution of near-pure-sterile solar neutrino oscillations plus near-pure-active atmospheric neutrino oscillations, the pure *CP* violation effect in $\Delta P(\nu_\mu \to \nu_\tau)$ is very small (~ 0.01) and is comparable to the matter effect. For $\nu_\mu \to \nu_e$ oscillation, the pure *CP* violation effect is independent of the active-sterile admixture and is at most 0.05 in $E=1.5-3$ GeV at $L=290$ km and the matter effect is at the 15–30 % level.

DOI: 10.1103/PhysRevD.65.073027 PACS number(s): 14.60.Pq, 11.30.Er, 14.60.Lm, 14.60.St

I. INTRODUCTION

CP violation has not yet been observed in the leptonic sector. Since it is found in the hadronic sector, such as in *K* [1] and *B* meson [2] decays, the observation of *CP* violation in neutrino oscillations will bring an important clue to understanding the origin of *CP* violation.

The solar neutrino deficit [3] and the atmospheric neutrino anomaly [4] have been interpreted as evidence of neutrino oscillation. The relevant mass-squared differences of the neutrinos are derived to be $\Delta m^2_{\rm atm}=(1.5-5)\times 10^{-3}$ eV^2 for the atmospheric neutrino anomaly [5] and to be in the range $\Delta m^2_{\rm solar}=(10^{-11}-10^{-4})$ eV^2, corresponding to the four solutions to the solar neutrino deficit [6]. Moreover, the Liquid Scintillation Neutrino Detector (LSND) measurements [7] have given possible evidence of $\nu_\mu \to \nu_e$ and $\overline{\nu}_\mu \to \overline{\nu}_e$ oscillations with $\Delta m^2_{\rm LSND}=(0.2-1)$ eV^2 in the short-baseline experiments.

The recent measurement of the solar neutrino flux by the use of ν_e charged current process on deuteron disintegration by the Sudbury Neutrino Observatory (SNO) [8] seems to indicate that the large mixing angle (LMA) solution and the low mass (LOW) solution in the Mikheyev-Smirnov-Wolfenstein (MSW) mechanism survive among the neutrino oscillation solutions for the solar neutrino problem in the three-neutrino mixing scheme [9].

As for the sterile neutrino [10–19], the oscillation into sterile neutrinos is claimed to be disfavored by the Super-Kamiokande Collaboration for both the solar neutrino [20] and the atmospheric neutrino [21] transitions in the two-neutrino analyses. However, the recent four-neutrino analyses by Barger, Marfatia, and Whisnant [22] and by Gonzalez-Garcia, Maltoni, and Peña-Garay [23] including the SNO measurement show that the oscillation into the active-sterile admixture is allowed for both the solar neutrino and the atmospheric neutrino.

CP violation in the long-baseline neutrino oscillations has been investigated in the three-neutrino mixing scheme [24–29], including the earth matter effect [30]. The size of the *CP* violation effects turns out to be of (a few-10)% level up to the neutrino energy $E\sim 1$ GeV at a baseline $L=250-730$ km for the mass-squared differences $\Delta m^2_{21}\equiv\Delta m^2_{\rm solar}\simeq 3\times 10^{-5}$ eV^2, $\Delta m^2_{31}\equiv\Delta m^2_{\rm atm}\simeq 3\times 10^{-3}$ eV^2 and $|U_{e3}|\simeq 0.05$ which is related to the only undetermined angle at present of the three mixing angles [27]. The matter effect affects the pure *CP* violation effect, depending on the length of the baseline, although there are cases in which the oscillation probabilities are approximately independent of the presence of matter, called ''vacuum mimicking phenomena'' [31]. The observability of the *CP* violation effects in long-baseline experiments was recently extensively studied for both the beams from the neutrino factory [32] and the conventional superbeams [33].

*Email address: hattori@ias.tokushima-u.ac.jp
†Email address: hasuike@anan-nct.ac.jp
‡Email address: wakaizum@medsci.tokushima-u.ac.jp

 ©2002 The American Physical Society

On the other hand, the CP violation effect in the four-neutrino mixing scheme with one sterile neutrino is shown to be possibly highly sizable [34] and is studied by us for its dependence on the mixing angles and phases for various oscillations such as $\nu_e \to \nu_\mu$ and $\nu_\mu \to \nu_\tau$ and is shown to reach to a magnitude as large as 0.3 in the $\nu_\mu \to \nu_\tau$ oscillation in the long-baseline experiments [35]. Since the oscillation pattern is governed by the LSND mass scale in the short-baseline experiments in the four-neutrino mixing scheme, the sensitivity to CP violation at the neutrino factory is studied in detail at the baseline $L = 10 - 100$ km [36,37].

In this paper we will investigate in the four-neutrino model how large the CP violation effects can be in the long-baseline experiments with $L = 290$ km and 730 km for Gonzalez-Garcia *et al.*'s two solutions [23], that is, (A) close-to-active solar neutrino oscillations plus close-to-sterile atmospheric neutrino oscillations and (B) near-pure-sterile solar neutrino oscillations plus near-pure-active atmospheric neutrino oscillations, and will evaluate the matter effect to these CP violation effects in the four-neutrino mixing scheme.

The paper is organized as follows. In Sec. II the method of calculating the oscillation probability with matter effect, formulated by Arafune, Koike, and Sato [25], is applied to the four-neutrino model. In Sec. III the constraints on the four-neutrino mixing matrix are derived by using the results from the recent combined analyses of the solar and atmospheric neutrino deficits in the four-neutrino scheme [23] and using the data from the LSND, Bugey, CHOOZ, CHORUS, and NOMAD experiments. In Sec. IV we study the behavior of the CP violation effect with respect to the mixing angle that governs the active-sterile admixture and, therefore, distinguishes the above-mentioned two solutions (A) and (B), and we show our results on the pure CP violation effects and the matter effect in the long-baseline experiments for $\nu_\mu \to \nu_e$ and $\nu_\mu \to \nu_\tau$ oscillations with the baselines of $L = 290$ km and 730 km. It turns out that the CP violation effect in $\nu_\mu \to \nu_\tau$ oscillation can be highly sizable (~ 0.2) for the solution (A) and is very small (~ 0.02) for the solution (B). On the other hand, the matter effect is small for $\nu_\mu \to \nu_e$ oscillation in the neutrino energy range $E \leqslant 2$ GeV at $L = 290$ km. For $\nu_\mu \to \nu_\tau$ oscillation, the matter effect is negligibly small in $E \leqslant 12$ GeV at $L = 730$ km for the solution (A), while it is comparable to pure CP violation effect for the solution (B). Section V is devoted to the conclusion.

II. OSCILLATION PROBABILITY IN THE FOUR-NEUTRINO MODEL

In order to consider the solar neutrino deficit, the atmospheric neutrino anomaly and the LSND experiment, we take the four-neutrino model with the three ordinary active neutrinos and one sterile neutrino with three different scales of the neutrino mass-squared difference, $\Delta m^2_{\rm solar} = (10^{-6} - 10^{-4})$ eV^2, $\Delta m^2_{\rm atm} = (1.5-5) \times 10^{-3}$ eV^2, and $\Delta m^2_{\rm LSND} = (0.2-1)$ eV^2.

Under the notion of the neutrino oscillation hypothesis [38,39], the flavor eigenstates of neutrinos ν_α ($\alpha = e, \mu, \tau, s$) are the mixtures of mass eigenstates in the vacuum ν_i ($i = 1,2,3,4$) with masses m_i as follows:

$$\nu_\alpha = \sum_{i=1}^{4} U^{(0)}_{\alpha i} \nu_i , \tag{1}$$

where ν_e, ν_μ, and ν_τ are the ordinary neutrinos, ν_s is the sterile neutrino, and $U^{(0)}$ is the unitary mixing matrix.

In order to evaluate the matter effect, which gives a fake CP violation effect, in the long-baseline neutrino oscillation experiments, we apply the method formulated by Arafune, Koike, and Sato [25] to the four-neutrino mixing scheme.

The evolution equation for the flavor eigenstate vector in matter is expressed as

$$i \frac{d\nu}{dx} = H \nu, \tag{2}$$

where x is the time in which the neutrino propagates and

$$\begin{aligned} H &\equiv - U \, \mathrm{diag}(p_1, p_2, p_3, p_4) U^\dagger \\ &\simeq \frac{1}{2E} U \, \mathrm{diag}(\mu_1^2, \mu_2^2, \mu_3^2, \mu_4^2) U^\dagger, \end{aligned} \tag{3}$$

with a unitary mixing matrix U, energy of neutrino E, and the effective mass squared μ_i^2's ($i = 1,2,3,4$). In Eq. (3) we have taken an approximation that neutrino masses are much smaller than their momenta and energies and have neglected an irrelevant term to the neutrino oscillation. The matrix U and the masses μ_i's are determined by

$$\begin{aligned} & U \begin{pmatrix} \mu_1^2 & 0 & 0 & 0 \\ 0 & \mu_2^2 & 0 & 0 \\ 0 & 0 & \mu_3^2 & 0 \\ 0 & 0 & 0 & \mu_4^2 \end{pmatrix} U^\dagger \\ &= U^{(0)} \begin{pmatrix} 0 & 0 & 0 & 0 \\ 0 & \Delta m^2_{21} & 0 & 0 \\ 0 & 0 & \Delta m^2_{31} & 0 \\ 0 & 0 & 0 & \Delta m^2_{41} \end{pmatrix} U^{(0)\dagger} \\ &\quad + \begin{pmatrix} a & 0 & 0 & 0 \\ 0 & 0 & 0 & 0 \\ 0 & 0 & 0 & 0 \\ 0 & 0 & 0 & a' \end{pmatrix}, \end{aligned} \tag{4}$$

where $\Delta m^2_{ij} = m_i^2 - m_j^2$ and

$$\begin{aligned} a &\equiv 2\sqrt{2} G_F N_e E = 7.60 \times 10^{-5} \frac{\rho}{(\mathrm{g\ cm^{-3}})} \frac{E}{(\mathrm{GeV})} \ \mathrm{eV}^2, \\ a' &\equiv \sqrt{2} G_F N_n E \simeq \sqrt{2} G_F N_e E = a/2. \end{aligned} \tag{5}$$

The quantities a and a' denote the matter effect to the oscillation, a coming from the charged current process of ν_e and a' from the neutral current process of ν_e, ν_μ, and ν_τ. In

Eq. (5), N_e is the electron density of the matter, ρ is the matter density, and N_n is the neutron density which is approximately equal to N_e since we consider the earth matter effect in the long-baseline experiments. The solution of Eq. (2) is given by

$$\nu(x)=S(x)\nu(0), \tag{6}$$

with

$$S(x)=T\exp\left(-i\int_0^x dsH(s)\right), \tag{7}$$

where T is the time ordering operator, and x is actually the distance in which the neutrino propagates with a speed almost equal to the light velocity. In the following, the matter density is assumed to be independent of space and time for simplicity, and then we have

$$S(x)=e^{-iHx}. \tag{8}$$

The oscillation probability for $\nu_\alpha\rightarrow\nu_\beta$ for the distance L is expressed as

$$P(\nu_\alpha\rightarrow\nu_\beta;L)=|S_{\beta\alpha}(L)|^2. \tag{9}$$

The oscillation probability for the antineutrinos $P(\overline{\nu}_\alpha\rightarrow\overline{\nu}_\beta;L)$ is obtained by replacing $U\rightarrow U^*$, $a\rightarrow -a$, and $a'\rightarrow -a'$ in Eq. (9). The CP violation effect in the neutrino oscillation is given by the probability difference between CP-conjugate channels as follows:

$$\Delta P(\nu_\alpha\rightarrow\nu_\beta)\equiv P(\nu_\alpha\rightarrow\nu_\beta;L)-P(\overline{\nu}_\alpha\rightarrow\overline{\nu}_\beta;L). \tag{10}$$

This quantity $\Delta P(\nu_\alpha\rightarrow\nu_\beta)$ consists of the pure CP-violation effect due to the phases of $U^{(0)}$ and the fake CP-violation effect due to the matter effect.

In the four-neutrino model, the four neutrino masses can be divided into two classes: 3+1 and 2+2 schemes. The 2+2 scheme consists of the two pairs of close masses separated by the LSND mass gap of the order of 1 eV [13,17,18] so as to accommodate the solar and atmospheric neutrino deficits and the LSND experiments together with the results from the other accelerator and reactor experiments on the neutrino oscillation. The 3+1 scheme consists of a group of three masses separated from an isolated one by the gap of the order of 1 eV. This scheme is only marginally allowed [40] and the phenomenology including CP violation is discussed by Donini and Maloni [37] together with the 2+2 scheme, showing that the detailed comparison of the physical reach of the neutrino factory in the two schemes gives similar results for the sensitivity to the mixing angles. We concentrate here on the 2+2 scheme in ordr to see the CP violation effect in the oscillation for various rates of the active-sterile admixture of neutrinos, as stated in the Introduction. There are the following two mass patterns in the 2+2 scheme: (i) $\Delta m^2_{\rm solar}\equiv\Delta m^2_{21}\ll\Delta m^2_{\rm atm}\equiv\Delta m^2_{43}\ll\Delta m^2_{\rm LSND}\equiv\Delta m^2_{32}$ and (ii) $\Delta m^2_{\rm solar}\equiv\Delta m^2_{43}\ll\Delta m^2_{\rm atm}\equiv\Delta m^2_{21}\ll\Delta m^2_{\rm LSND}\equiv\Delta m^2_{32}$. We will adopt the first pattern in the following analyses, and the second pattern can be attained only through the exchange of indices $(1,2)\leftrightarrow(3,4)$ in the following various expressions such as the oscillation probabilities.

Since $\Delta m^2_{21}\ll\Delta m^2_{31},\Delta m^2_{41}$ and $a,a'\ll\Delta m^2_{31},\Delta m^2_{41}$, we decompose H as $H=H_0+H_1$ of Eq. (3) with

$$H_0=\frac{1}{2E}U^{(0)}\begin{pmatrix}0&0&0&0\\0&0&0&0\\0&0&\Delta m^2_{31}&0\\0&0&0&\Delta m^2_{41}\end{pmatrix}U^{(0)\dagger}, \tag{11}$$

and

$$H_1=\frac{1}{2E}U^{(0)}\begin{pmatrix}0&0&0&0\\0&\Delta m^2_{21}&0&0\\0&0&0&0\\0&0&0&0\end{pmatrix}U^{(0)\dagger}+\frac{1}{2E}\begin{pmatrix}a&0&0&0\\0&0&0&0\\0&0&0&0\\0&0&0&a'\end{pmatrix}, \tag{12}$$

and treat H_1 as a perturbation and calculate Eq. (8) up to the first order in a, a', and Δm^2_{21}. Following the Arafune-Koike-Sato procedure [25], $S(x)$ of Eq. (8) is given by

$$S(x)\simeq e^{-iH_0x}-ie^{-iH_0x}\int_0^x dsH_1(s), \tag{13}$$

where $H_1(x)=e^{iH_0x}H_1e^{-iH_0x}$. The approximation in Eq. (13) requires

$$\frac{\Delta m^2_{21}L}{2E}\ll 1,\quad \frac{aL}{2E}\ll 1,\quad \frac{a'L}{2E}\ll 1. \tag{14}$$

The requirements of Eq. (14) are satisfied for $\Delta m^2_{21}=(10^{-5}-10^{-4})$ eV^2, $\Delta m^2_{31}=(0.1-1)$ eV^2, $E=1-15$ GeV, $L=(300-750)$ km, and $\rho=3$ g/cm^3 as

$$\frac{\Delta m^2_{21}L}{2E}\simeq 5\times 10^{-4}-0.2,\quad \frac{aL}{2E},\ \frac{a'L}{2E}\simeq 0.1-0.4. \tag{15}$$

Equation (14) also shows that the approximation becomes better as the energy E increases, so we can apply this approximation to the multi-GeV region such as $E=1-15$ GeV. If we express $S_{\beta\alpha}(x)$ as

$$S_{\beta\alpha}(x)=\delta_{\beta\alpha}+iT_{\beta\alpha}(x), \tag{16}$$

then $iT_{\beta\alpha}(x)$ is obtained as follows (in the following, $U^{(0)}_{\beta\alpha}$ is denoted as $U_{\beta\alpha}$ for brevity):

$$
\begin{aligned}
iT_{\beta\alpha}(x) = & -2i\exp\left(-i\frac{\Delta m_{31}^2 x}{4E}\right)\sin\left(\frac{\Delta m_{31}^2 x}{4E}\right)\Bigg[U_{\beta 3}U_{\alpha 3}^*\Bigg\{1-\frac{a}{\Delta m_{31}^2}(2|U_{e3}|^2-\delta_{\alpha e}-\delta_{\beta e}) \\
& -\frac{a'}{\Delta m_{31}^2}(2|U_{s3}|^2-\delta_{\alpha s}-\delta_{\beta s})-i\frac{ax}{2E}|U_{e3}|^2-i\frac{a'x}{2E}|U_{s3}|^2\Bigg\} \\
& -\left(\frac{a}{\Delta m_{31}^2}+\frac{a}{\Delta m_{43}^2}\right)(U_{\alpha 3}^*U_{\beta 4}U_{e3}U_{e4}^*+U_{\alpha 4}^*U_{\beta 3}U_{e4}U_{e3}^*) \\
& -\left(\frac{a'}{\Delta m_{31}^2}+\frac{a'}{\Delta m_{43}^2}\right)(U_{\alpha 3}^*U_{\beta 4}U_{s3}U_{s4}^*+U_{\alpha 4}^*U_{\beta 3}U_{s4}U_{s3}^*)\Bigg]-2i\exp\left(-i\frac{\Delta m_{41}^2 x}{4E}\right)\sin\left(\frac{\Delta m_{41}^2 x}{4E}\right) \\
& \times\Bigg[U_{\beta 4}U_{\alpha 4}^*\Bigg\{1-\frac{a}{\Delta m_{41}^2}(2|U_{e4}|^2-\delta_{\alpha e}-\delta_{\beta e})-\frac{a'}{\Delta m_{41}^2}(2|U_{s4}|^2-\delta_{\alpha s}-\delta_{\beta s})-i\frac{ax}{2E}|U_{e4}|^2-i\frac{a'x}{2E}|U_{s4}|^2\Bigg\} \\
& -\left(\frac{a}{\Delta m_{41}^2}-\frac{a}{\Delta m_{43}^2}\right)(U_{\alpha 3}^*U_{\beta 4}U_{e3}U_{e4}^*+U_{\alpha 4}^*U_{\beta 3}U_{e4}U_{e3}^*) \\
& -\left(\frac{a'}{\Delta m_{41}^2}-\frac{a'}{\Delta m_{43}^2}\right)(U_{\alpha 3}^*U_{\beta 4}U_{s3}U_{s4}^*+U_{\alpha 4}^*U_{\beta 3}U_{s4}U_{s3}^*)\Bigg] \\
& -i\frac{\Delta m_{31}^2 x}{2E}\Bigg[\frac{\Delta m_{21}^2}{\Delta m_{31}^2}U_{\beta 2}U_{\alpha 2}^*+\frac{a}{\Delta m_{31}^2}\{\delta_{\alpha e}\delta_{\beta e}+U_{\beta 3}U_{\alpha 3}^*(2|U_{e3}|^2-\delta_{\alpha e}-\delta_{\beta e})+U_{\beta 4}U_{\alpha 4}^*(2|U_{e4}|^2-\delta_{\alpha e}-\delta_{\beta e}) \\
& +U_{\alpha 3}^*U_{\beta 4}U_{e3}U_{e4}^*+U_{\alpha 4}^*U_{\beta 3}U_{e4}U_{e3}^*\}+\frac{a'}{\Delta m_{31}^2}\{\delta_{\alpha s}\delta_{\beta s}+U_{\beta 3}U_{\alpha 3}^*(2|U_{s3}|^2-\delta_{\alpha s}-\delta_{\beta s}) \\
& +U_{\beta 4}U_{\alpha 4}^*(2|U_{s4}|^2-\delta_{\alpha s}-\delta_{\beta s})+U_{\alpha 3}^*U_{\beta 4}U_{s3}U_{s4}^*+U_{\alpha 4}^*U_{\beta 3}U_{s4}U_{s3}^*\}\Bigg]. \qquad (17)
\end{aligned}
$$

We use Eq. (17) in Eq. (16) and calculate the oscillation probability for $\nu_\alpha \to \nu_\beta$ by Eq. (9). The complete expression of $P(\nu_\alpha \to \nu_\beta; L)$ in the four-neutrino model with matter effect is given in the Appendix.

III. CONSTRAINTS ON THE MIXING MATRIX

In this section the constraints imposed on the mixing matrix U are derived from the solar neutrino deficit, atmospheric neutrino anomaly, LSND experiments and the other terrestrial oscillation experiments using the accelerators and reactors.

(i) We use the results of the recent combined analysis of the atmospheric neutrino anomaly and the solar neutrino deficit in the four-neutrino scheme, done by Gonzalez-Garcia, Maltoni, and Peña-Garay [23]. They obtained two solutions: (A) close-to-active solar neutrino oscillations plus close-to-sterile atmospheric neutrino oscillations, expressed by

$$|U_{s1}|^2+|U_{s2}|^2 \sim 0.2, \qquad (18)$$

and (B) near-pure-sterile solar neutrino oscillations plus near-pure-active atmospheric neutrino oscillations, expressed by

$$|U_{s1}|^2+|U_{s2}|^2 \sim 0.91-0.97. \qquad (19)$$

For the later convenience, we define the quantity $|U_{s1}|^2+|U_{s2}|^2$ as D.

(ii) A constraint on $U_{\mu 3}$ and $U_{\mu 4}$ is derived from the atmospheric neutrino anomaly, where the survival probability of ν_μ is given by

$$
\begin{aligned}
P(\nu_\mu \to \nu_\mu) \simeq & 1-4|U_{\mu 3}|^2|U_{\mu 4}|^2\sin^2\Delta_{43} \\
& -2(|U_{\mu 1}|^2+|U_{\mu 2}|^2)(1-|U_{\mu 1}|^2-|U_{\mu 2}|^2), \qquad (20)
\end{aligned}
$$

where $\Delta_{ij} \equiv \Delta m_{ij}^2 L/(4E)$. The Super-Kamiokande data, $\sin^2 2\theta_{\rm atm} > 0.82$ for $5\times 10^{-4} < \Delta m_{\rm atm}^2 < 6\times 10^{-3}$ eV^2 [4], give a constraint, along with the expectation of $|U_{\mu 1}|^2+|U_{\mu 2}|^2 \ll 1$, of

$$|U_{\mu 3}|^2|U_{\mu 4}|^2 > 0.205. \qquad (21)$$

(iii) The Bugey experiment of short-baseline reactor $\bar{\nu}_e$ disappearance [41] gives a constraint on $|U_{e3}|^2+|U_{e4}|^2$. The survival probability of $\bar{\nu}_e$ is expressed by

$$P(\bar{\nu}_e\to\bar{\nu}_e)\simeq 1-4(|U_{e3}|^2+|U_{e4}|^2)\times(1-|U_{e3}|^2-|U_{e4}|^2)\sin^2\Delta_{32}, \quad (22)$$

where $\Delta_{41}\sim\Delta_{42}\sim\Delta_{31}\sim\Delta_{32}$ is used. The data, $\sin^2 2\theta_{\rm Bugey}<0.1$ for $0.1<\Delta m^2<1$ eV^2, bring a constraint of

$$|U_{e3}|^2+|U_{e4}|^2<0.025. \quad (23)$$

The first long-baseline reactor experiment, that is, the CHOOZ experiment [42] gives a constraint of $4|U_{e3}|^2|U_{e4}|^2<0.18$, through their data of $\sin^2 2\theta_{\rm CHOOZ}<0.18$ for $3\times10^{-3}<\Delta m^2<1.0\times10^{-2}$ eV^2. This constraint can be involved in the constraint of Eq. (23) obtained from the Bugey experiment.

(iv) In the same way as above, the LSND experiment [7] brings a constraint of

$$|U^*_{\mu3}U_{e3}+U^*_{\mu4}U_{e4}|=0.016-0.12 \quad (24)$$

from the data of $\sin^2 2\theta_{\rm LSND}=1.0\times10^{-3}-6.0\times10^{-2}$ for $0.2<\Delta m^2_{\rm LSND}<2$ eV^2.

(v) The CHORUS [43] and NOMAD [44] experiments searching for the $\nu_\mu\to\nu_\tau$ oscillation gives a constraint of

$$|U^*_{\mu3}U_{\tau3}+U^*_{\mu4}U_{\tau4}|<0.4 \quad (25)$$

for $\Delta m^2<1$ eV^2, which is derived from the latest NOMAD experimental data of $\sin^2 2\theta_{\rm NOMAD}<(0.8\ {\rm eV}^2/\Delta m^2)^2$ for $0.8<\Delta m^2<10$ eV^2.

The details of the derivation of the constraints in (ii)–(v) can be seen in our previous work [35].

IV. *CP* VIOLATION AND MATTER EFFECT

In this section we will investigate how large the *CP* violation effect could be in the long-baseline neutrino oscillations in the light of the recent combined analysis of the solar and atmospheric neutrino deficits, that is, depending on the rate of the active-sterile neutrino admixture, and how much the matter effect affects the pure *CP* violation effect.

In order to translate the constraints on U derived in the previous section into the ones with the mixing angles and phases, we adopt the most general parametrization of U for Majorana neutrinos [19], which includes six mixing angles and six phases. The expression of the matrix is too complicated to show here, so that we cite only the matrix elements which are useful for the following analyses: $U_{e1}=c_{01}c_{02}c_{03}$, $U_{e2}=c_{02}c_{03}s^*_{d01}$, $U_{e3}=c_{03}s^*_{d02}$, $U_{e4}=s^*_{d03}$, $U_{\mu3}=-s^*_{d02}s_{d03}s^*_{d13}+c_{02}c_{13}s^*_{d12}$, $U_{\mu4}=c_{03}s^*_{d13}$, $U_{\tau3}=-c_{13}s^*_{d02}s_{d03}s^*_{d23}-c_{02}s^*_{d12}s_{d13}s^*_{d23}+c_{02}c_{12}c_{23}$, $U_{\tau4}=c_{03}c_{13}s^*_{d23}$, $U_{s3}=-c_{13}s^*_{d02}s_{d03}c_{23}-c_{02}s^*_{d12}s_{d13}c_{23}-c_{02}c_{12}s_{d23}$, and $U_{s4}=c_{03}c_{13}c_{23}$ (instead of U_{s1} and U_{s2}), where $c_{ij}\equiv\cos\theta_{ij}$ and $s_{dij}\equiv s_{ij}e^{i\delta_{ij}}\equiv\sin\theta_{ij}e^{i\delta_{ij}}$, and $\theta_{01},\theta_{02},\theta_{03},\theta_{12},\theta_{13},\theta_{23}$ are the six angles and $\delta_{01},\delta_{02},\delta_{03},\delta_{12},\delta_{13},\delta_{23}$ are the six phases. Three of the six oscillation probability differences are independent so that only three of the six phases are determined by the measurements of the *CP* violation effects, that is, the Dirac phases.

By using this parametrization of U, the constraints of Eqs. (18), (19), (21), (23), (24) and (25) are expressed by the mixing angles and phases as follows:

$$|s_{02}s_{03}c_{13}c_{23}e^{-i\delta_1}+c_{02}c_{23}s_{12}s_{13}+c_{02}c_{12}s_{23}e^{i\delta_2}|^2+|c_{03}c_{13}c_{23}|^2\sim0.8\quad({\rm A})\quad{\rm or}\quad0.03-0.09\quad({\rm B}), \quad (26)$$

$$|-s_{02}s_{03}s_{13}e^{-i\delta_1}+c_{02}c_{13}s_{12}|^2c^2_{03}s^2_{13}>0.205, \quad (27)$$

$$c^2_{03}s^2_{02}+s^2_{03}<0.025, \quad (28)$$

$$|c_{02}s_{02}c_{03}s_{12}c_{13}+c^2_{02}c_{03}s_{03}s_{13}e^{i\delta_1}|=0.016-0.12, \quad (29)$$

$$|c^2_{02}c_{12}s_{12}c_{13}c_{23}-c_{02}s_{02}s_{03}s_{12}c^2_{13}s_{23}e^{-i(\delta_1+\delta_2)}-c_{02}s_{02}s_{03}c_{12}s_{13}c_{23}e^{i\delta_1}+c_{02}s_{02}s_{03}s_{12}s^2_{13}s_{23}e^{i(\delta_1-\delta_2)}+c_{13}s_{13}s_{23}(c^2_{03}-c^2_{02}s^2_{12}+s^2_{02}s^2_{03})e^{-i\delta_2}|<0.4, \quad (30)$$

where $\delta_1\equiv\delta_{02}-\delta_{03}-\delta_{12}+\delta_{13}$ and $\delta_2\equiv\delta_{12}-\delta_{13}+\delta_{23}$. The constraint of Eq. (26) is expressed for $|U_{s3}|^2+|U_{s4}|^2$ instead of the one for $|U_{s1}|^2+|U_{s2}|^2$ in Eqs. (18) and (19).

Equation (28) from the Bugey experiment gives a stringent constraint on the two mixing angles s_{02} and s_{03}, like the one for $|U_{e3}|$ from the CHOOZ experiment in the three-neutrino mixing scheme. And, in this situation, Eq. (27) from the atmospheric neutrinos gives a strong constraint on the mixing angles s_{12} and s_{13}, roughly $s_{12}>0.91$ and s_{13} around the maximal mixing. The angle s_{23} strongly affects the rate of the active-sterile admixture, $|U_{s1}|^2+|U_{s2}|^2$ $(\equiv D)$, as seen in Eq. (26). The angle s_{01} does not occur in Eqs. (26)–(30). The phase δ_1 affects the the determination of the allowed regions of s_{02}, s_{03}, s_{12}, and s_{13} through Eqs. (27) and (29).

In order to see the gross features of the pure *CP* violation effect in the long-baseline $\nu_\mu\to\nu_e$ and $\nu_\mu\to\nu_\tau$ oscillations with respect to the mixing angles and phases, we write down the expressions of the effect to the leading terms relevant to the long-baseline oscillation and by using the smallness of s_{02} and s_{03} as follows:

$$\Delta P(\nu_\mu\to\nu_e)\simeq 4c_{02}s_{02}c^2_{03}s_{03}s_{12}c_{13}s_{13}\times\sin\delta_1\sin\left(\frac{\Delta m^2_{43}L}{2E}\right), \quad (31)$$

$$\Delta P(\nu_\mu\to\nu_\tau)\simeq -4c^2_{02}c^2_{03}c_{12}s_{12}c^2_{13}s_{13}c_{23}s_{23}\times\sin\delta_2\sin\left(\frac{\Delta m^2_{43}L}{2E}\right). \quad (32)$$

These expressions are obtained from the exact expression of the pure *CP* violation effect of Eq. (10), not from the approximate one given in the Appendix. As can be seen in Eqs. (31) and (32), $\Delta P(\nu_\mu\to\nu_e)$ depends primarily on the phase

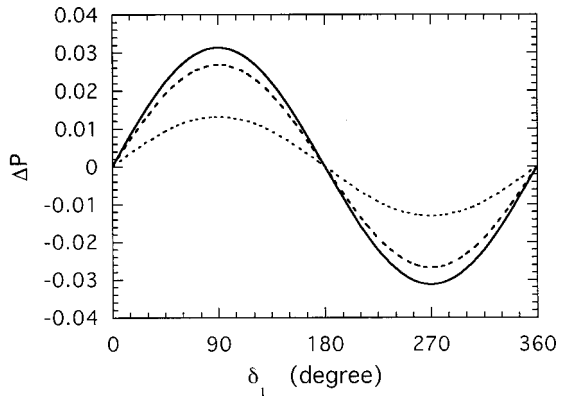

FIG. 1. The pure CP violation effect in $\nu_\mu \to \nu_e$ oscillation with respect to the phase δ_1 of the mixing matrix in the long-baseline experiment with the baseline $L=290$ km and the neutrino energy $E=1.2$ GeV for the typical three parameter sets: ($s_{02}=0.12$, $s_{03}=0.06$, $s_{12}=0.93$, $s_{13}=0.71$) (solid line), ($s_{02}=0.12$, $s_{03}=0.05$, $s_{12}=0.97$, $s_{13}=0.71$) (dashed line), and ($s_{02}=0.15$, $s_{03}=0.02$, $s_{12}=0.95$, $s_{13}=0.71$) (dotted line), and commonly taken as $s_{01}=s_{23}=1/\sqrt{2}$, $\delta_{01}=\delta_{02}=\delta_{03}=\delta_{12}=0$, and $\delta_2=\pi/2$. The mass-squared differences of neutrinos are fixed as $\Delta m^2_{\rm atm}=2.5\times10^{-3}$ eV^2, $\Delta m^2_{\rm LSND}=0.3$ eV^2, and $\Delta m^2_{\rm solar}=5\times10^{-5}$ eV^2.

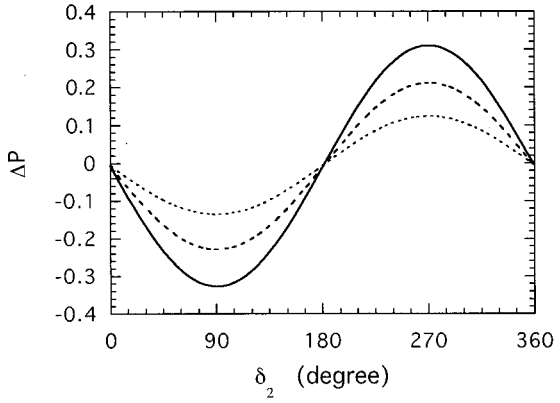

FIG. 2. The pure CP violation effect in $\nu_\mu \to \nu_\tau$ oscillation with respect to the phase δ_2 of the mixing matrix in the long-baseline experiment with the baseline $L=730$ km and the neutrino energy $E=6.1$ GeV for the typical three parameter sets: ($s_{02}=0.12$, $s_{03}=0.06$, $s_{12}=0.93$, $s_{13}=0.71$) (solid line), ($s_{02}=0.12$, $s_{03}=0.06$, $s_{12}=0.97$, $s_{13}=0.71$) (dashed line), and ($s_{02}=0.15$, $s_{03}=0.03$, $s_{12}=0.99$, $s_{13}=0.71$) (dotted line), and commonly taken as $s_{01}=s_{23}=1/\sqrt{2}$, $\delta_{01}=\delta_{02}=\delta_{03}=\delta_{12}=0$, and $\delta_1=\pi/2$. The mass-squared differences of neutrinos are the same as in Fig. 1.

δ_1 and $\Delta P(\nu_\mu \to \nu_\tau)$ depends on the phase δ_2. The angle s_{23} determines $\Delta P(\nu_\mu \to \nu_\tau)$, but does not affect $\Delta P(\nu_\mu \to \nu_e)$ to the leading terms. Similarly, the angles s_{02} and s_{03} determine $\Delta P(\nu_\mu \to \nu_e)$, but do not appreciably affect $\Delta P(\nu_\mu \to \nu_\tau)$, since s_{02} and s_{03} are very small. So, first, in Fig. 1 we show the pure CP violation effect in $\nu_\mu \to \nu_e$ oscillation as a function of the phase δ_1 for the baseline of $L=290$ km and the neutrino energy $E=1.2$ GeV for the typical three parameter sets which are allowed by the constraints of Eqs. (26)–(30): ($s_{02}=0.12$, $s_{03}=0.06$, $s_{12}=0.93$, $s_{13}=0.71$), ($s_{02}=0.12$, $s_{03}=0.05$, $s_{12}=0.97$, $s_{13}=0.71$), and ($s_{02}=0.15$, $s_{03}=0.02$, $s_{12}=0.95$, $s_{13}=0.71$), and commonly $s_{01}=s_{23}=1/\sqrt{2}$ and $\delta_2=\pi/2$. We have taken the mass-squared differences as $\Delta m^2_{43}=\Delta m^2_{\rm atm}=2.5\times10^{-3}$ eV^2, $\Delta m^2_{32}=\Delta m^2_{\rm LSND}=0.3$ eV^2, and $\Delta m^2_{21}=\Delta m^2_{\rm solar}=5\times10^{-5}$ eV^2, which are fixed in the following unless stated otherwise. As seen in Fig. 1, the magnitude of CP violation in $\nu_\mu \to \nu_e$ oscillation is at most 0.03 for $L=290$ km and at $E=1.2$ GeV, which is almost the same in magnitude as in the three-neutrino mixing scheme. In Fig. 2 we show the pure CP violation effect in $\nu_\mu \to \nu_\tau$ oscillation as a function of the phase δ_2 at $L=730$ km and $E=6.1$ GeV for the typical three parameter sets: ($s_{02}=0.12$, $s_{03}=0.06$, $s_{12}=0.93$, $s_{13}=0.71$), ($s_{02}=0.12$, $s_{03}=0.06$, $s_{12}=0.97$, $s_{13}=0.71$), and ($s_{02}=0.15$, $s_{03}=0.03$, $s_{12}=0.99$, $s_{13}=0.71$), and commonly $s_{01}=s_{23}=1/\sqrt{2}$ and $\delta_1=\pi/2$. As seen in Fig. 2, the magnitude of CP violation effect in $\nu_\mu \to \nu_\tau$ oscillation could attain as large as 0.3, as already shown in Ref. [35]. We show in Fig. 3 the pure CP violation effect in $\nu_\mu \to \nu_\tau$ oscillation as a function of the mixing angle θ_{23} at $L=730$ km and $E=6.1$ GeV for the three parameter sets: ($s_{02}=s_{03}=0.11$, $s_{12}=0.93$, $s_{13}=0.71$), ($s_{02}=0.15$, $s_{03}=0.05$, $s_{12}=0.95$, $s_{13}=0.71$), and ($s_{02}=s_{03}=0.11$, $s_{12}=0.97$, $s_{13}=0.71$), and commonly $s_{01}=1/\sqrt{2}$ and $\delta_1=\delta_2=\pi/2$. As seen in Fig. 3, the maximal mixing of $\theta_{23}(\simeq 45°)$ gives the maximum CP violation effect. As can be seen fron Eqs. (31)and (32), the CP violation effects $\Delta P(\nu_\mu \to \nu_e)$ and $\Delta P(\nu_\mu \to \nu_\tau)$ do not depend on the mixing angle s_{01} to the leading terms. So, in the following calculations we fix as $s_{01}=1/\sqrt{2}$.

Next, we discuss the relation between the rate of active-sterile admixture $|U_{s1}|^2+|U_{s2}|^2$ ($\equiv D$) and the pure CP violation effect in $\nu_\mu \to \nu_e$ and $\nu_\mu \to \nu_\tau$ oscillations, where D is given by Eq. (26) subtracted from 1. As can be seen from Eq. (31), since the pure CP violation effect $\Delta P(\nu_\mu \to \nu_e)$ does not depend on the mixing angle s_{23} to the leading terms, it does not vary with the quantity D. So, $\Delta P(\nu_\mu \to \nu_e)$ is

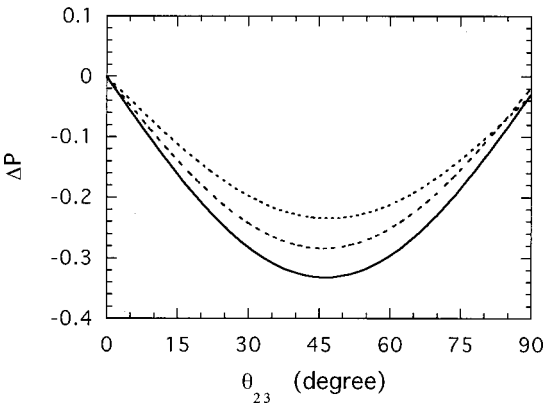

FIG. 3. The pure CP violation effect in $\nu_\mu \to \nu_\tau$ oscillation with respect to the mixing angle θ_{23} of the mixing matrix at $L=730$ km and $E=6.1$ GeV for the typical three parameter sets: ($s_{02}=s_{03}=0.11$, $s_{12}=0.93$, $s_{13}=0.71$) (solid line), ($s_{02}=0.15$,$s_{03}=0.05$, $s_{12}=0.95$, $s_{13}=0.71$) (dashed line), and ($s_{02}=s_{03}=0.11$, $s_{12}=0.97$, $s_{13}=0.71$) (dotted line), and commonly taken as $s_{01}=1/\sqrt{2}$, $\delta_{01}=\delta_{02}=\delta_{03}=\delta_{12}=0$, and $\delta_1=\delta_2=\pi/2$.

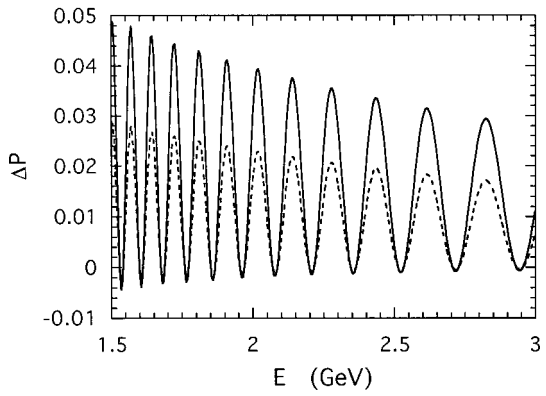

FIG. 4. The pure *CP* violation effect in $\nu_\mu \to \nu_e$ oscillation with respect to the neutrino energy $E(=1.5$–3 GeV) at $L=290$ km for the typical two parameter sets: ($s_{02}=s_{03}=0.11$, $s_{12}=0.97$, $s_{13}=0.73$) (solid line) and ($s_{02}=0.12$, $s_{03}=0.06$, $s_{12}=0.93$, $s_{13}=0.71$) (dashed line), and commonly taken as $s_{01}=1/\sqrt{2}$, $s_{23}=0.4$, $\delta_{01}=\delta_{02}=\delta_{03}=\delta_{12}=0$, and $\delta_1=\delta_2=\pi/2$.

almost the same at the level of $\leqslant 0.05$ at $L=290$ km and in $1 \leqslant E \leqslant 10$ GeV among the close-to-active solar neutrino oscillations plus close-to-sterile atmospheric neutrino oscillations ($D \sim 0.2$), near-pure-sterile solar neutrino oscillations plus near-pure-active atmospheric neutrino oscillations ($D \sim 0.91-0.97$), and the maximal active-sterile admixture ($D \sim 0.5$). We show in Fig. 4 the pure *CP* violation effect of $\Delta P(\nu_\mu \to \nu_e)$ at $L=290$ km in the neutrino energy range of $1.5 \leqslant E \leqslant 3$ GeV for the two cases of mixing angles: ($s_{02}=s_{03}=0.11$, $s_{12}=0.97$, $s_{13}=0.73$) in solid line and ($s_{02}=0.12$, $s_{03}=0.06$, $s_{12}=0.93$, $s_{13}=0.71$) in dashed line, for commonly $s_{23}=0.4$ and $\delta_1=\delta_2=\pi/2$. In order to see the magnitude of the matter effect to $\Delta P(\nu_\mu \to \nu_e)$, we show in Figs. 5 and 6 the pure *CP* violation effect (solid line) and the matter effect (dotted line) for the above-mentioned two cases of the mixing angles, respectively. The matter effect is calculated from the equation in the Appendix and, as can be seen in Figs. 5 and 6, its relative magnitude to the pure *CP* violation effect is around 15% at 1.5 GeV and 30% at 3 GeV. Figure 7 shows the pure *CP* violation effect and the matter effect in $\nu_\mu \to \nu_e$ oscillation in the high energy range of $3 \leqslant E \leqslant 10$ GeV for ($s_{02}=s_{03}=0.11$, $s_{12}=0.97$, $s_{13}=0.73$). The relative magnitude of the matter effect becomes larger than that in the energy range of $1.5 \leqslant E \leqslant 3$ GeV.

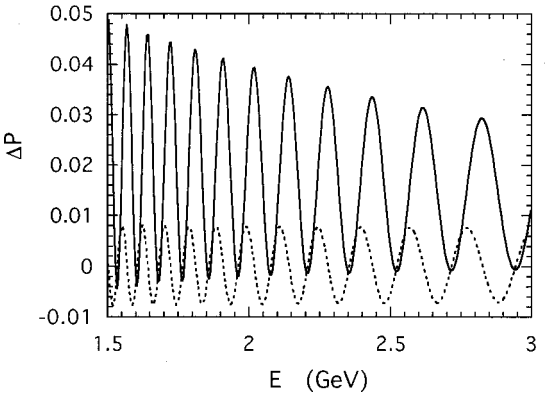

FIG. 5. The pure *CP* violation effect (solid line) and the matter effect (dotted line) in $\nu_\mu \to \nu_e$ oscillation with respect to the neutrino energy E at $L=290$ km for the parameter set ($s_{02}=s_{03}=0.11$, $s_{12}=0.97$, $s_{13}=0.73$) and the other angles and phases are the same as in Fig. 4.

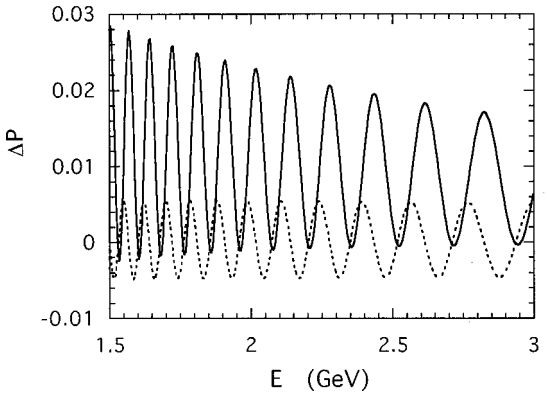

FIG. 6. The pure *CP* violation effect (solid line) and the matter effect (dotted line) in $\nu_\mu \to \nu_e$ oscillation with respect to the neutrino energy E at $L=290$ km for the parameter set ($s_{02}=0.12$,$s_{03}=0.06$,$s_{12}=0.93$,$s_{13}=0.71$) and the other angles and phases are the same as in Fig. 4.

For $\nu_\mu \to \nu_\tau$ oscillation, the pure *CP* violation effect $\Delta P(\nu_\mu \to \nu_\tau)$ depends on s_{23} as can be seen from Eq. (32) and therefore on the quantity D. In Tables I–III, we show $\Delta P(\nu_\mu \to \nu_\tau)$ as a function of the mixing angle s_{23} and the phase δ_2, both of which largely affect the magnitude of D, at $L=730$ km and $E=6.1$ GeV for the typical three cases of (s_{02},s_{03},s_{12},s_{13}). The case of ($s_{02}=0.12$, $s_{03}=0.06$, $s_{12}=0.93$, $s_{13}=0.71$) and $\delta_2=90°$ gives a class of the possibly maximum values of $\Delta P(\nu_\mu \to \nu_\tau)$ at that baseline and neutrino energy in the region of the mixing angles and phases allowed by Eqs. (26)–(30). In Figs. 8–12 we show the relation between the rate of active-sterile admixture D and the behavior of the *CP* violation effect in the $\nu_\mu \to \nu_\tau$ oscillation at $L=730$ km in the energy range $6 \leqslant E \leqslant 15$ GeV. In the

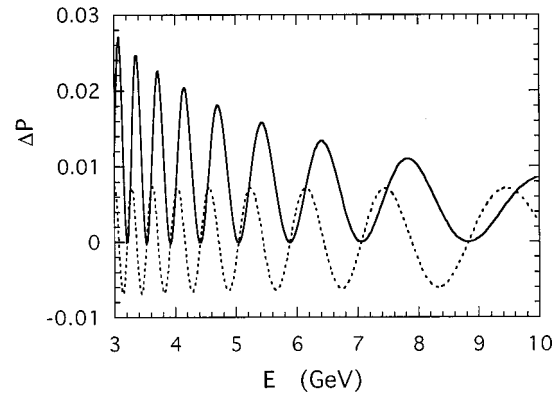

FIG. 7. The pure *CP* violation effect (solid line) and the matter effect (dotted line) in $\nu_\mu \to \nu_e$ oscillation in the energy range $E=3$–10 GeV at $L=290$ km for the parameter set ($s_{02}=s_{03}=0.11$, $s_{12}=0.97$, $s_{13}=0.73$) and the other angles and phases are the same as in Fig. 4.

TABLE I. The pure CP violation effect in $\nu_\mu \to \nu_\tau$ oscillation, $\Delta P(\nu_\mu \to \nu_\tau)$, at the baseline $L=730$ km and neutrino energy $E=6.1$ GeV, and the active-sterile admixture D with respect to the mixing angle s_{23} and the phase δ_2 for the parameter set of ($s_{02}=0.12$, $s_{03}=0.06$, $s_{12}=0.93$, $s_{13}=0.71$) and $\delta_1=\pi/2$.

	$\delta_2=30°$		$\delta_2=60°$		$\delta_2=90°$	
s_{23}	D	$\Delta P(\nu_\mu \to \nu_\tau)$	D	$\Delta P(\nu_\mu \to \nu_\tau)$	D	$\Delta P(\nu_\mu \to \nu_\tau)$
0.00	0.08	0.00	0.08	0.00	0.08	0.00
0.10	0.04	-0.03	0.06	-0.06	0.08	-0.06
0.20	0.03	-0.06	0.06	-0.11	0.11	-0.13
0.30	0.03	-0.09	0.08	-0.16	0.15	-0.18
0.40	0.05	-0.12	0.12	-0.20	0.20	-0.24
0.50	0.10	-0.14	0.17	-0.24	0.28	-0.28
0.60	0.16	-0.16	0.25	-0.27	0.36	-0.31
0.65	0.21	-0.16	0.29	-0.28	0.41	-0.32
0.70	0.26	-0.17	0.35	-0.28	0.47	-0.33
0.75	0.32	-0.17	0.40	-0.28	0.52	-0.32
0.80	0.38	-0.16	0.47	-0.28	0.58	-0.32
0.85	0.46	-0.15	0.54	-0.26	0.65	-0.30
0.90	0.55	-0.14	0.62	-0.23	0.72	-0.26
0.95	0.67	-0.11	0.72	-0.18	0.79	-0.21
1.00	0.87	-0.02	0.87	-0.02	0.87	-0.02

TABLE III. The pure CP violation effect in $\nu_\mu \to \nu_\tau$ oscillation, $\Delta P(\nu_\mu \to \nu_\tau)$, at $L=730$ km and $E=6.1$ GeV, and the active-sterile admixture D with respect to the mixing angle s_{23} and the phase δ_2 for the parameter set of ($s_{02}=0.12$, $s_{03}=0.06$, $s_{12}=0.99$, $s_{13}=0.73$) and $\delta_1=\pi/2$.

	$\delta_2=30°$		$\delta_2=60°$		$\delta_2=90°$	
s_{23}	D	$\Delta P(\nu_\mu \to \nu_\tau)$	D	$\Delta P(\nu_\mu \to \nu_\tau)$	D	$\Delta P(\nu_\mu \to \nu_\tau)$
0.00	0.02	0.00	0.02	0.00	0.02	0.00
0.10	0.01	-0.013	0.02	-0.02	0.03	-0.03
0.20	0.02	-0.025	0.04	-0.04	0.06	-0.05
0.30	0.06	-0.038	0.08	-0.06	0.11	-0.07
0.40	0.11	-0.049	0.14	-0.08	0.17	-0.10
0.50	0.18	-0.059	0.22	-0.10	0.26	-0.11
0.60	0.28	-0.067	0.32	-0.11	0.37	-0.13
0.65	0.34	-0.070	0.38	-0.12	0.43	-0.13
0.70	0.40	-0.072	0.44	-0.12	0.49	-0.14
0.75	0.47	-0.072	0.51	-0.12	0.56	-0.14
0.80	0.55	-0.072	0.59	-0.12	0.64	-0.13
0.85	0.64	-0.069	0.67	-0.11	0.71	-0.13
0.90	0.73	-0.064	0.76	-0.10	0.80	-0.11
0.95	0.84	-0.054	0.86	-0.08	0.89	-0.09
1.00	0.98	-0.019	0.98	-0.02	0.98	-0.02

case of the solution of the close-to-active solar neutrino oscillations plus close-to-sterile atmospheric neutrino oscillations ($D\sim 0.2$) to the combined analysis of the solar and atmospheric neutrinos [23], the pure CP violation effect of $\Delta P(\nu_\mu \to \nu_\tau)$ is shown in Fig. 8 for the two cases of ($s_{02}=0.12$, $s_{03}=0.06$, $s_{12}=0.93$, $s_{13}=0.71$, $s_{23}=0.40$) and ($s_{02}=0.12$, $s_{03}=0.06$, $s_{12}=0.97$, $s_{13}=0.72$, $s_{23}=0.40$), along with the matter effect for the first case of the above two cases. The first case represents the possibly maximum value of the pure $\Delta P(\nu_\mu \to \nu_\tau)$ for this solution ($D\sim 0.2$). The matter effect is around 8% at 6 GeV and 15% at 10 GeV relative to the pure CP violation effects, and is about half the one of the $\nu_\mu \to \nu_e$ oscillation. Figure 9 shows the pure CP violation effect (solid line) and the magnitude of the matter effect (dotted line) for the second case of the above two cases. The matter effect is very small in $6 \leqslant E \leqslant 12$ GeV in comparison with the pure CP violation effect. We show in

TABLE II. The pure CP violation effect in $\nu_\mu \to \nu_\tau$ oscillation, $\Delta P(\nu_\mu \to \nu_\tau)$, at $L=730$ km and $E=6.1$ GeV, and the active-sterile admixture D with respect to the mixing angle s_{23} and the phase δ_2 for the parameter set of ($s_{02}=0.12$, $s_{03}=0.06$, $s_{12}=0.97$, $s_{13}=0.72$) and $\delta_1=\pi/2$.

	$\delta_2=30°$		$\delta_2=60°$		$\delta_2=90°$	
s_{23}	D	$\Delta P(\nu_\mu \to \nu_\tau)$	D	$\Delta P(\nu_\mu \to \nu_\tau)$	D	$\Delta P(\nu_\mu \to \nu_\tau)$
0.00	0.04	0.00	0.04	0.00	0.04	0.00
0.10	0.02	-0.02	0.03	-0.04	0.05	-0.04
0.20	0.02	-0.04	0.04	-0.07	0.08	-0.09
0.30	0.04	-0.06	0.07	-0.11	0.12	-0.13
0.40	0.08	-0.08	0.12	-0.14	0.18	-0.16
0.50	0.14	-0.10	0.19	-0.17	0.27	-0.19
0.60	0.23	-0.11	0.28	-0.19	0.37	-0.21
0.65	0.28	-0.11	0.34	-0.19	0.42	-0.22
0.70	0.34	-0.12	0.40	-0.20	0.48	-0.23
0.75	0.40	-0.12	0.46	-0.20	0.55	-0.23
0.80	0.48	-0.11	0.54	-0.19	0.62	-0.22
0.85	0.56	-0.11	0.62	-0.18	0.69	-0.21
0.90	0.66	-0.10	0.71	-0.16	0.77	-0.19
0.95	0.77	-0.08	0.80	-0.13	0.85	-0.15
1.00	0.94	-0.02	0.94	-0.02	0.94	-0.02

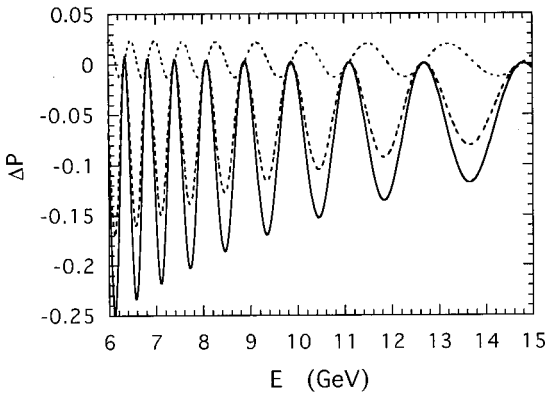

FIG. 8. The pure CP violation effect in $\nu_\mu \to \nu_\tau$ oscillation in the energy range of $E=6$–15 GeV at $L=730$ km for the typical two parameter sets: ($s_{02}=0.12$, $s_{03}=0.06$, $s_{12}=0.93$, $s_{13}=0.71$, $s_{23}=0.40$) (solid line) and ($s_{02}=0.12$, $s_{03}=0.06$, $s_{12}=0.97$, $s_{13}=0.72$, $s_{23}=0.40$) (dashed line) for the active-sterile admixture $D\sim 0.2$, and the matter effect (dotted line) for the first parameter set of the above, and commonly taken as $s_{01}=1/\sqrt{2}$, $\delta_{01}=\delta_{02}=\delta_{03}=\delta_{12}=0$, and $\delta_1=\delta_2=\pi/2$.

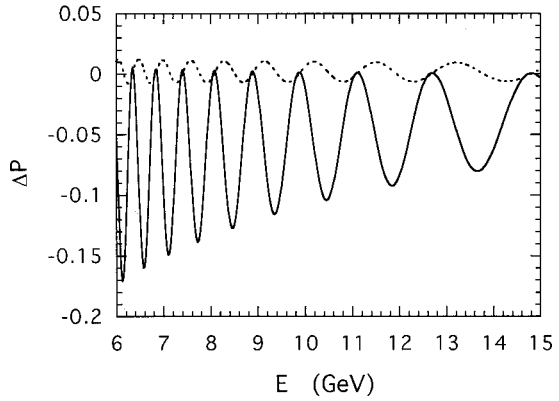

FIG. 9. The pure *CP* violation effect (solid line) and the matter effect (dotted line) in $\nu_\mu \to \nu_\tau$ oscillation at $L=730$ km for the parameter set, ($s_{02}=0.12$, $s_{03}=0.06$, $s_{12}=0.97$, $s_{13}=0.72$, $s_{23}=0.40$) and the other angles and phases are the same as in Fig. 8.

Fig. 10 the pure $\Delta P(\nu_\mu \to \nu_\tau)$ and the matter effect for the solution of the near-pure-sterile solar neutrino oscillations plus near-pure-active atmospheric neutrino oscillations ($D \sim 0.91-0.97$) for the typical case of ($s_{02}=0.12$, $s_{03}=0.06$, $s_{12}=0.95$,$s_{13}=0.71$,$s_{23}=1.0$). The pure *CP* violation effect is very small, ~ -0.01, and is comparable to the matter effect.

Incidentally, we show in Fig. 11 the pure $\Delta P(\nu_\mu \to \nu_\tau)$ and the matter effect for the case of the maximal active-sterile admixture ($D \sim 0.5$), which is not allowed by the combined analysis of the solar and atmospheric neutrinos [23], for the two parameter sets of ($s_{02}=0.12$, $s_{03}=0.06$, $s_{12}=0.93$, $s_{13}=0.71$, $s_{23}=0.75$) and ($s_{02}=0.12$, $s_{03}=0.06$, $s_{12}=0.97$, $s_{13}=0.73$, $s_{23}=0.70$), along with the matter effect for the first set. The first parameter set represents the possibly maximum value of the pure $\Delta P(\nu_\mu \to \nu_\tau)$ in this case. Figure 12 shows the pure *CP* violation effect (solid line) and the matter effect (dotted line) for the second set of the above two sets. The matter effect is very small in $6 \leqslant E \leqslant 15$ GeV in comparison with the pure *CP* violation effect.

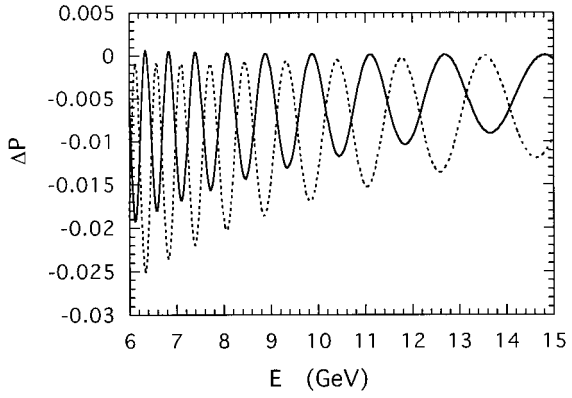

FIG. 10. The pure *CP* violation effect (solid line) and the matter effect (dotted line) for the active-sterile admixture $D \sim 0.9$ in $\nu_\mu \to \nu_\tau$ oscillation at $L=730$ km for the parameter set, ($s_{02}=0.12$, $s_{03}=0.06$, $s_{12}=0.95$, $s_{13}=0.71$, $s_{23}=1.0$) and taken as $s_{01}=1/\sqrt{2}$, $\delta_{01}=\delta_{02}=\delta_{03}=\delta_{12}=0$, and $\delta_1=\delta_2=\pi/2$.

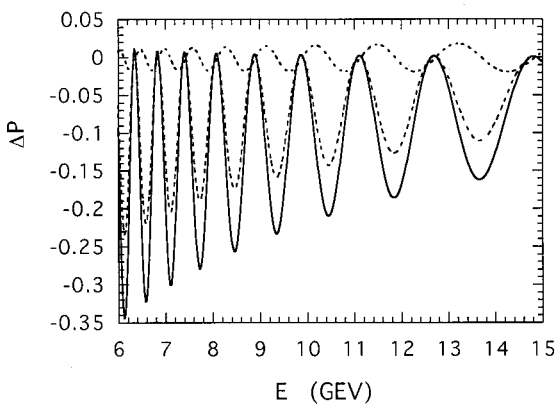

FIG. 11. The pure *CP* violation effect in $\nu_\mu \to \nu_\tau$ oscillation at $L=730$ km for the typical two parameter sets ($s_{02}=0.12$, $s_{03}=0.06$, $s_{12}=0.93$, $s_{13}=0.71$, $s_{23}=0.75$) (solid line) and ($s_{02}=0.12$, $s_{03}=0.06$, $s_{12}=0.97$, $s_{13}=0.73$, $s_{23}=0.70$) (dashed line) for the maximal active-sterile admixture $D \sim 0.5$, and the matter effect (dotted line) for the first parameter set of the above, and commonly taken as $s_{01}=1/\sqrt{2}$, $\delta_{01}=\delta_{02}=\delta_{03}=\delta_{12}=0$, and $\delta_1=\delta_2=\pi/2$.

V. CONCLUSION

We have evaluated the pure *CP* violation effect and the fake one due to the matter effect in the long-baseline neutrino oscillations for the baselines $L=290$ km and 730 km in the neutrino energy range $E=1.5-15$ GeV in the four-neutrino model with the 2+2 scheme, where two pairs of two close neutrino masses are separated by the LSND mass gap of the order of 1 eV, on the basis of the constraints on the mixing matrix from the solar neutrino deficit, atmospheric neutrino anomaly, LSND experiments, Bugey and CHOOZ measurements, and CHORUS and NOMAD experiments. The matter effect is estimated with Arafune-Koike-Sato's approximation method [25]. The matter effect is at $(15-30)\%$ level, relative to the pure *CP* violation effect for $\nu_\mu \to \nu_e$ oscillation in $1.5 \leqslant E \leqslant 3$ GeV at $L=290$ km, and is at $(8-15)\%$ level for $\nu_\mu \to \nu_\tau$ oscillation in $6 \leqslant E \leqslant 10$ GeV at $L=730$ km for the active-sterile admixture

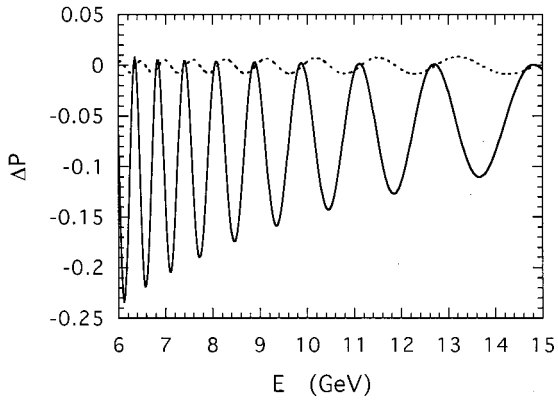

FIG. 12. The pure *CP* violation effect (solid line) and the matter effect (dotted line) in $\nu_\mu \to \nu_\tau$ oscillation at $L=730$ km for the parameter set ($s_{02}=0.12$, $s_{03}=0.06$, $s_{12}=0.97$, $s_{13}=0.73$, $s_{23}=0.70$) and the other angles and phases are the same as in Fig. 11.

range of $0.15 \leqslant D \leqslant 0.8$, where $D \equiv |U_{s1}|^2 + |U_{s2}|^2$.

Then, we have studied the relation between the active-sterile admixture (D) of neutrinos and the magnitude of pure CP violation effect. For the close-to-active solar neutrino oscillations plus close-to-sterile atmospheric neutrino oscillations ($D \sim 0.2$) [23], the pure CP violation effect in $\Delta P(\nu_\mu \to \nu_\tau)$ could attain the magnitude as large as 0.10–0.25 in $6 \leqslant E \leqslant 15$ GeV at $L = 730$ km for $\Delta m^2_{\rm atm} = 2.5 \times 10^{-3}$ eV^2, $\Delta m^2_{\rm solar} = 5 \times 10^{-5}$ eV^2 and $\Delta m^2_{\rm LSND} = 0.3$ eV^2. This magnitude is prominently governed by the mixing angle product $c_{23}s_{23}$ in $\Delta P(\nu_\mu \to \nu_\tau)$, and s_{23} determines the active-sterile admixture D. For near-pure-sterile solar neutrino oscillations plus near-pure-active atmospheric neutrino oscillations ($D \sim 0.91 - 0.97$) [23], the pure CP violation effect in $\Delta P(\nu_\mu \to \nu_\tau)$ is very small, about 0.01, in $6 \leqslant E \leqslant 15$ GeV at $L = 730$ km and is comparable to the matter effect. On the other hand, for $\nu_\mu \to \nu_e$ oscillation, the pure CP violation effect is independent of the active-sterile admixture and is at most 0.05 in $1.5 \leqslant E \leqslant 3$ GeV at $L = 290$ km, which is almost the same in magnitude as in the three-neutrino model.

It may be interesting to measure the CP violation effect in $\nu_\mu \to \nu_\tau$ oscillation for the baseline of $L = 730$ km by using the conventional superbeams of ν_μ and $\overline{\nu_\mu}$ in the energy range of $E = 6 - 15$ GeV [45,46]. Also it might be intriguing to measure the CP violation effect in $\nu_\mu \to \nu_e$ oscillation for $L = 250 - 300$ km by using the conventional superbeams of ν_μ and $\overline{\nu_\mu}$ in $E = 0.1 - 3$ GeV [47].

APPENDIX: OSCILLATION PROBABILITY

Here we present the oscillation probability of Eq. (9) with Eq. (17) taken in Eq. (16):

$$
\begin{aligned}
P(\nu_\alpha \to \nu_\beta; L) = \delta_{\beta\alpha} \Bigg[& 1 - 4 \sin^2\left(\frac{\Delta m^2_{31} L}{4E}\right) \Bigg\{ |U_{\alpha 3}|^2 \Bigg[1 - 2\frac{a}{\Delta m^2_{31}}(|U_{e3}|^2 - \delta_{\alpha e}) - 2\frac{a'}{\Delta m^2_{31}}(|U_{s3}|^2 - \delta_{\alpha s}) \Bigg] \\
& - 2\left(\frac{a}{\Delta m^2_{31}} + \frac{a}{\Delta m^2_{43}}\right) \mathrm{Re}(U^*_{\alpha 3} U_{\alpha 4} U_{e3} U^*_{e4}) - 2\left(\frac{a'}{\Delta m^2_{31}} + \frac{a'}{\Delta m^2_{43}}\right) \mathrm{Re}(U^*_{\alpha 3} U_{\alpha 4} U_{s3} U^*_{s4}) \Bigg\} \\
& - 2 \sin\left(\frac{\Delta m^2_{31} L}{2E}\right) |U_{\alpha 3}|^2 \left(\frac{aL}{2E} |U_{e3}|^2 + \frac{a'L}{2E} |U_{s3}|^2 \right) - 4 \sin^2\left(\frac{\Delta m^2_{41} L}{4E}\right) \Bigg\{ |U_{\alpha 4}|^2 \\
& \times \Bigg[1 - 2\frac{a}{\Delta m^2_{41}}(|U_{e3}|^2 - \delta_{\alpha e}) - 2\frac{a'}{\Delta m^2_{41}}(|U_{s4}|^2 - \delta_{\alpha s}) \Bigg] - 2\left(\frac{a}{\Delta m^2_{41}} - \frac{a}{\Delta m^2_{43}}\right) \mathrm{Re}(U^*_{\alpha 3} U_{\alpha 4} U_{e3} U^*_{e4}) \\
& - 2\left(\frac{a'}{\Delta m^2_{41}} - \frac{a'}{\Delta m^2_{43}}\right) \mathrm{Re}(U^*_{\alpha 3} U_{\alpha 4} U_{s3} U^*_{s4}) \Bigg\} - 2 \sin\left(\frac{\Delta m^2_{41} L}{2E}\right) |U_{\alpha 4}|^2 \left(\frac{aL}{2E} |U_{e4}|^2 + \frac{a'L}{2E} |U_{s4}|^2 \right) \Bigg] \\
& + 4 \sin^2\left(\frac{\Delta m^2_{31} L}{4E}\right) \Bigg[|U_{\alpha 3}|^2 |U_{\beta 3}|^2 \Bigg\{ 1 - 2\frac{a}{\Delta m^2_{31}}(2|U_{e3}|^2 - \delta_{\alpha e} - \delta_{\beta e}) - 2\frac{a'}{\Delta m^2_{31}}(2|U_{s3}|^2 - \delta_{\alpha s} - \delta_{\beta s}) \Bigg\} \\
& - 2\left(\frac{a}{\Delta m^2_{31}} + \frac{a}{\Delta m^2_{43}}\right) \{ |U_{\alpha 3}|^2 \, \mathrm{Re}(U^*_{\beta 3} U_{\beta 4} U_{e3} U^*_{e4}) + |U_{\beta 3}|^2 \, \mathrm{Re}(U^*_{\alpha 3} U_{\alpha 4} U_{e3} U^*_{e4}) \} \\
& - 2\left(\frac{a'}{\Delta m^2_{31}} + \frac{a'}{\Delta m^2_{43}}\right) \{ |U_{\alpha 3}|^2 \, \mathrm{Re}(U^*_{\beta 3} U_{\beta 4} U_{s3} U^*_{s4}) + |U_{\beta 3}|^2 \, \mathrm{Re}(U^*_{\alpha 3} U_{\alpha 4} U_{s3} U^*_{s4}) \} \Bigg] \\
& + 2\frac{\Delta m^2_{31} L}{2E} \sin\left(\frac{\Delta m^2_{31} L}{2E}\right) \Bigg[\frac{\Delta m^2_{21}}{\Delta m^2_{31}} \mathrm{Re}(U^*_{\beta 3} U_{\beta 2} U_{\alpha 3} U^*_{\alpha 2}) + \frac{a}{\Delta m^2_{31}} \{ |U_{e3}|^2 \delta_{\alpha e} \delta_{\beta e} \\
& + |U_{\alpha 3}|^2 |U_{\beta 3}|^2 (2|U_{e3}|^2 - \delta_{\alpha e} - \delta_{\beta e}) + \mathrm{Re}(U^*_{\beta 3} U_{\beta 4} U_{\alpha 3} U^*_{\alpha 4}) \\
& \times (2|U_{e4}|^2 - \delta_{\alpha e} - \delta_{\beta e}) + |U_{\alpha 3}|^2 \, \mathrm{Re}(U^*_{\beta 3} U_{\beta 4} U_{e3} U^*_{e4}) + |U_{\beta 3}|^2 \, \mathrm{Re}(U^*_{\alpha 3} U_{\alpha 4} U_{e3} U^*_{e4}) \} \\
& + \frac{a'}{\Delta m^2_{31}} \{ |U_{s3}|^2 \delta_{\alpha s} \delta_{\beta s} + |U_{\alpha 3}|^2 |U_{\beta 3}|^2 (2|U_{s3}|^2 - \delta_{\alpha s} - \delta_{\beta s}) + \mathrm{Re}(U^*_{\beta 3} U_{\beta 4} U_{\alpha 3} U^*_{\alpha 4}) \\
& \times (2|U_{s4}|^2 - \delta_{\alpha s} - \delta_{\beta s}) + |U_{\alpha 3}|^2 \, \mathrm{Re}(U^*_{\beta 3} U_{\beta 4} U_{s3} U^*_{s4}) + |U_{\beta 3}|^2 \, \mathrm{Re}(U^*_{\alpha 3} U_{\alpha 4} U_{s3} U^*_{s4}) \} \Bigg] \Bigg]
\end{aligned}
$$

$$
-4\frac{\Delta m_{31}^2 L}{2E}\sin^2\left(\frac{\Delta m_{31}^2 L}{4E}\right)\left[\frac{\Delta m_{21}^2}{\Delta m_{31}^2}\mathrm{Im}(U_{\beta 3}^* U_{\beta 2} U_{\alpha 3} U_{\alpha 2}^*)\right.
$$

$$
+\frac{a}{\Delta m_{31}^2}\{\mathrm{Im}(U_{\beta 3}^* U_{\beta 4} U_{\alpha 3} U_{\alpha 4}^*)\times(2|U_{e4}|^2-\delta_{\alpha e}-\delta_{\beta e})+|U_{\alpha 3}|^2\,\mathrm{Im}(U_{\beta 3}^* U_{\beta 4} U_{e3} U_{e4}^*)
$$

$$
-|U_{\beta 3}|^2\,\mathrm{Im}(U_{\alpha 3}^* U_{\alpha 4} U_{e3} U_{e4}^*)\}+\frac{a'}{\Delta m_{31}^2}\{\mathrm{Im}(U_{\beta 3}^* U_{\beta 4} U_{\alpha 3} U_{\alpha 4}^*)(2|U_{s4}|^2-\delta_{\alpha s}-\delta_{\beta s})
$$

$$
\left.+|U_{\alpha 3}|^2\,\mathrm{Im}(U_{\beta 3}^* U_{\beta 4} U_{s3} U_{s4}^*)-|U_{\beta 3}|^2\,\mathrm{Im}(U_{\alpha 3}^* U_{\alpha 4} U_{s3} U_{s4}^*)\}\right]+4\sin^2\left(\frac{\Delta m_{41}^2 L}{4E}\right)
$$

$$
\times\left[|U_{\alpha 4}|^2|U_{\beta 4}|^2\left\{1-2\frac{a}{\Delta m_{41}^2}(2|U_{e4}|^2-\delta_{\alpha e}-\delta_{\beta e})-2\frac{a'}{\Delta m_{41}^2}(2|U_{s4}|^2-\delta_{\alpha s}-\delta_{\beta s})\right\}-2\left(\frac{a}{\Delta m_{41}^2}-\frac{a}{\Delta m_{43}^2}\right)\right.
$$

$$
\times\{|U_{\alpha 4}|^2\,\mathrm{Re}(U_{\beta 3}^* U_{\beta 4} U_{e3} U_{e4}^*)+|U_{\beta 4}|^2\,\mathrm{Re}(U_{\alpha 3}^* U_{\alpha 4} U_{e3} U_{e4}^*)\}-2\left(\frac{a'}{\Delta m_{41}^2}-\frac{a'}{\Delta m_{43}^2}\right)
$$

$$
\left.\times\{|U_{\alpha 4}|^2\,\mathrm{Re}(U_{\beta 3}^* U_{\beta 4} U_{s3} U_{s4}^*)+|U_{\beta 4}|^2\,\mathrm{Re}(U_{\alpha 3}^* U_{\alpha 4} U_{s3} U_{s4}^*)\}\right]+2\frac{\Delta m_{31}^2 L}{2E}\sin\left(\frac{\Delta m_{41}^2 L}{2E}\right)
$$

$$
\times\left[\frac{\Delta m_{21}^2}{\Delta m_{31}^2}\mathrm{Re}(U_{\beta 4}^* U_{\beta 2} U_{\alpha 4} U_{\alpha 2}^*)+\frac{a}{\Delta m_{31}^2}\{|U_{e4}|^2\delta_{\alpha e}\delta_{\beta e}+|U_{\alpha 4}|^2|U_{\beta 4}|^2(2|U_{e4}|^2-\delta_{\alpha e}-\delta_{\beta e})\right.
$$

$$
+\mathrm{Re}(U_{\beta 3}^* U_{\beta 4} U_{\alpha 3} U_{\alpha 4}^*)(2|U_{e3}|^2-\delta_{\alpha e}-\delta_{\beta e})+|U_{\alpha 4}|^2\,\mathrm{Re}(U_{\beta 3}^* U_{\beta 4} U_{e3} U_{e4}^*)+|U_{\beta 4}|^2\,\mathrm{Re}(U_{\alpha 3}^* U_{\alpha 4} U_{e3} U_{e4}^*)\}
$$

$$
+\frac{a'}{\Delta m_{31}^2}\{|U_{s4}|^2\delta_{\alpha s}\delta_{\beta s}+|U_{\alpha 4}|^2|U_{\beta 4}|^2(2|U_{s4}|^2-\delta_{\alpha s}-\delta_{\beta s})+\mathrm{Re}(U_{\beta 3}^* U_{\beta 4} U_{\alpha 3} U_{\alpha 4}^*)(2|U_{s3}|^2-\delta_{\alpha s}-\delta_{\beta s})
$$

$$
\left.+|U_{\alpha 4}|^2\,\mathrm{Re}(U_{\beta 3}^* U_{\beta 4} U_{s3} U_{s4}^*)+|U_{\beta 4}|^2\,\mathrm{Re}(U_{\alpha 3}^* U_{\alpha 4} U_{s3} U_{s4}^*)\}\right]-4\frac{\Delta m_{31}^2 L}{2E}\sin^2\left(\frac{\Delta m_{41}^2 L}{4E}\right)
$$

$$
\times\left[\frac{\Delta m_{21}^2}{\Delta m_{31}^2}\mathrm{Im}(U_{\beta 4}^* U_{\beta 2} U_{\alpha 4} U_{\alpha 2}^*)+\frac{a}{\Delta m_{31}^2}\{\mathrm{Im}(U_{\beta 4}^* U_{\beta 3} U_{\alpha 4} U_{\alpha 3}^*)(2|U_{e3}|^2-\delta_{\alpha e}-\delta_{\beta e})+|U_{\alpha 4}|^2\right.
$$

$$
\times\mathrm{Im}(U_{\beta 4}^* U_{\beta 3} U_{e4} U_{e3}^*)-|U_{\beta 4}|^2\,\mathrm{Im}(U_{\alpha 4}^* U_{\alpha 3} U_{e4} U_{e3}^*)\}
$$

$$
+\frac{a'}{\Delta m_{31}^2}\{\mathrm{Im}(U_{\beta 4}^* U_{\beta 3} U_{\alpha 4} U_{\alpha 3}^*)(2|U_{s3}|^2-\delta_{\alpha s}-\delta_{\beta s})
$$

$$
\left.+|U_{\alpha 4}|^2\,\mathrm{Im}(U_{\beta 4}^* U_{\beta 3} U_{s4} U_{s3}^*)-|U_{\beta 4}|^2\,\mathrm{Im}(U_{\alpha 4}^* U_{\alpha 3} U_{s4} U_{s3}^*)\}\right]
$$

$$
+8\sin\left(\frac{\Delta m_{31}^2 L}{4E}\right)\sin\left(\frac{\Delta m_{41}^2 L}{4E}\right)\cos\left(\frac{\Delta m_{43}^2 L}{4E}\right)\left[\mathrm{Re}(U_{\beta 3}^* U_{\beta 4} U_{\alpha 3} U_{\alpha 4}^*)\left\{1-\frac{a}{\Delta m_{31}^2}(2|U_{e3}|^2-\delta_{\alpha e}-\delta_{\beta e})\right.\right.
$$

$$
\left.-\frac{a}{\Delta m_{41}^2}(2|U_{e4}|^2-\delta_{\alpha e}-\delta_{\beta e})-\frac{a'}{\Delta m_{31}^2}(2|U_{s3}|^2-\delta_{\alpha s}-\delta_{\beta s})-\frac{a'}{\Delta m_{41}^2}(2|U_{s4}|^2-\delta_{\alpha s}-\delta_{\beta s})\right\}
$$

$$
+\mathrm{Im}(U_{\beta 3}^* U_{\beta 4} U_{\alpha 3} U_{\alpha 4}^*)\left(\frac{aL}{2E}|U_{e4}|^2+\frac{a'L}{2E}|U_{s4}|^2-\frac{aL}{2E}|U_{e3}|^2-\frac{a'L}{2E}|U_{s3}|^2\right)-\left(\frac{a}{\Delta m_{41}^2}-\frac{a}{\Delta m_{43}^2}\right)
$$

$$
\times\{|U_{\alpha 3}|^2\,\mathrm{Re}(U_{\beta 3}^* U_{\beta 4} U_{e3} U_{e4}^*)+|U_{\beta 3}|^2\,\mathrm{Re}(U_{\alpha 3}^* U_{\alpha 4} U_{e3} U_{e4}^*)\}-\left(\frac{a'}{\Delta m_{41}^2}-\frac{a'}{\Delta m_{43}^2}\right)
$$

$$\times\{|U_{\alpha3}|^2\,\mathrm{Re}(U^*_{\beta3}U_{\beta4}U_{s3}U^*_{s4})+|U_{\beta3}|^2\,\mathrm{Re}(U^*_{\alpha3}U_{\alpha4}U_{s3}U^*_{s4})\}-\left(\frac{a}{\Delta m^2_{31}}+\frac{a}{\Delta m^2_{43}}\right)$$

$$\times\{|U_{\alpha4}|^2\,\mathrm{Re}(U^*_{\beta3}U_{\beta4}U_{e3}U^*_{e4})+|U_{\beta4}|^2\,\mathrm{Re}(U^*_{\alpha3}U_{\alpha4}U_{e3}U^*_{e4})\}-\left(\frac{a'}{\Delta m^2_{31}}+\frac{a'}{\Delta m^2_{43}}\right)$$

$$\times\{|U_{\alpha4}|^2\,\mathrm{Re}(U^*_{\beta3}U_{\beta4}U_{s3}U^*_{s4})+|U_{\beta4}|^2\,\mathrm{Re}(U^*_{\alpha3}U_{\alpha4}U_{s3}U^*_{s4})\}\Bigg]$$

$$+8\sin\left(\frac{\Delta m^2_{31}L}{4E}\right)\sin\left(\frac{\Delta m^2_{41}L}{4E}\right)\sin\left(\frac{\Delta m^2_{43}L}{4E}\right)\Bigg[\mathrm{Im}(U^*_{\beta3}U_{\beta4}U_{\alpha3}U^*_{\alpha4})\Bigg\{1-\frac{a}{\Delta m^2_{31}}(2|U_{e3}|^2-\delta_{\alpha e}-\delta_{\beta e})$$

$$-\frac{a}{\Delta m^2_{41}}(2|U_{e4}|^2-\delta_{\alpha e}-\delta_{\beta e})-\frac{a'}{\Delta m^2_{31}}(2|U_{s3}|^2-\delta_{\alpha s}-\delta_{\beta s})-\frac{a'}{\Delta m^2_{41}}(2|U_{s4}|^2-\delta_{\alpha s}-\delta_{\beta s})\Bigg\}$$

$$-\mathrm{Re}(U^*_{\beta3}U_{\beta4}U_{\alpha3}U^*_{\alpha4})\left(\frac{aL}{2E}|U_{e4}|^2+\frac{a'L}{2E}|U_{s4}|^2-\frac{aL}{2E}|U_{e3}|^2-\frac{a'L}{2E}|U_{s3}|^2\right)-\left(\frac{a}{\Delta m^2_{41}}-\frac{a}{\Delta m^2_{43}}\right)$$

$$\times\{|U_{\alpha3}|^2\,\mathrm{Im}(U^*_{\beta3}U_{\beta4}U_{e3}U^*_{e4})-|U_{\beta3}|^2\,\mathrm{Im}(U^*_{\alpha3}U_{\alpha4}U_{e3}U^*_{e4})\}-\left(\frac{a'}{\Delta m^2_{41}}-\frac{a'}{\Delta m^2_{43}}\right)$$

$$\times\{|U_{\alpha3}|^2\,\mathrm{Im}(U^*_{\beta3}U_{\beta4}U_{s3}U^*_{s4})-|U_{\beta3}|^2\,\mathrm{Im}(U^*_{\alpha3}U_{\alpha4}U_{s3}U^*_{s4})\}-\left(\frac{a}{\Delta m^2_{31}}+\frac{a}{\Delta m^2_{43}}\right)$$

$$\times\{|U_{\alpha4}|^2\,\mathrm{Im}(U^*_{\beta3}U_{\beta4}U_{e3}U^*_{e4})-|U_{\beta4}|^2\,\mathrm{Im}(U^*_{\alpha3}U_{\alpha4}U_{e3}U^*_{e4})\}-\left(\frac{a'}{\Delta m^2_{31}}+\frac{a'}{\Delta m^2_{43}}\right)$$

$$\times\{|U_{\alpha4}|^2\,\mathrm{Im}(U^*_{\beta3}U_{\beta4}U_{s3}U^*_{s4})-|U_{\beta4}|^2\,\mathrm{Im}(U^*_{\alpha3}U_{\alpha4}U_{s3}U^*_{s4})\}\Bigg].$$

[1] J. H. Christenson, J. W. Cronin, V. L. Fitch, and R. Turlay, Phys. Rev. Lett. **13**, 138 (1964).

[2] BABAR Collaboration, B. Aubert *et al.*, Phys. Rev. Lett. **87**, 091801 (2001); Belle Collaboration, K. Abe *et al.*, *ibid.* **87**, 091802 (2001).

[3] B. T. Cleveland, T. Daily, R. Davis, J. R. Distel, K. Lande, C. K. Lee, P. S. Wildenhain, and J. Ullman, Astrophys. J. **496**, 505 (1988); R. Davis, Prog. Part. Nucl. Phys. **32**, 13 (1994); K. Lande, P. Wildenhain, R. Corey, M. Foygel, and J. Distel, in *Neutrino 2000*, Proceedings of the 19th International Conference on Neutrino Physics and Astrophysics, Sudbury, 2000, edited by J. Law, R. W. Ollerhead, and J. J. Simpson [Nucl. Phys. B (Proc. Suppl.) **91**, 50 (2001)]; SAGE Collaboration, J. N. Abdurashitov *et al.* Phys. Rev. C **60**, 055801 (1999); SAGE Collaboration, V. Gavrin, in *Neutrino 2000*, Proceedings of the 19th International Conference on Neutrino Physics and Astrophysics, Sudbury, 2000, edited by J. Law, R. W. Ollerhead, and J. J. Simpson [Nucl. Phys. B (Proc. Suppl.) **91**, 36 (2001)]; GALLEX Collaboration, W. Hampel *et al.*, Phys. Lett. B **447**, 127 (1999); GNO Collaboration, M. Altmann *et al.*, *ibid.* **490**, 16 (2000); GNO Collaboration, E. Bellotti, in *Neutrino 2000*, Proceedings of the 19th International Conference on Neutrino Physics and Astrophysics, Sudbury, 2000, edited by J. Law, R. W. Ollerhead, and J. J. Simpson [Nucl. Phys. B (Proc. Suppl.) **91**, 44 (2001)]; Kamiokande Collaboration, Y. Fukuda *et al.*, Phys. Rev. Lett. **77**, 1683 (1996); Super-Kamiokande Collaboration, Y. Fukuda *et al.*, *ibid.* **81**, 1158 (1998); **81**, 4279(E) (1998); **82**, 1810 (1999); **82**, 2430 (1999); Super-Kamiokande Collaboration, Y. Suzuki, in *Neutrino 2000*, Proceedings of the 19th International Conference on Neutrino Physics and Astrophysics, Sudbury, 2000, edited by J. Law, R. W. Ollerhead, and J. J. Simpson [Nucl. Phys. B (Proc. Suppl.) **91**, 29 (2001)]; Super-Kamiokande Collaboration, S. Fukuda, Phys. Rev. Lett. **86**, 5651 (2001).

[4] Kamiokande Collaboration, K. S. Hirata *et al.*, Phys. Lett. B **205**, 416 (1988); Kamiokande Collaboration, Y. Fukuda *et al.*, *ibid.* **335**, 237 (1994); IMB Collaboration, D. Casper *et al.*, Phys. Rev. Lett. **66**, 2561 (1991); IMB Collaboration, R. Becker-Szendy *et al.*, Phys. Rev. D **46**, 3720 (1992); Soudan2 Collaboration, W. W. M. Allison *et al.*, Phys. Lett. B **391**, 491 (1997); Super-Kamiokande Collaboration, Y. Fukuda *et al.*, *ibid.* **433**, 9 (1998); **436**, 33 (1998); Phys. Rev. Lett. **82**, 2644 (1999); Super-Kamiokande Collaboration, T. Toshito, in *ICHEP 2000*, Proceedings of the 30th International Conference on High Energy Physics, Osaka, 2000, edited by C. S. Lim and T. Yamanaka (World Scientific, Singapore, 2001), p. 913; MACRO Collaboration, M. Ambrosio *et al.*, Phys. Lett. B **434**, 451 (1998).

[5] Super-Kamiokande Collaboration, Y. Fukuda *et al.*, Phys. Rev. Lett. **81**, 1562 (1998).
[6] J. N. Bahcall, P. I. Krastev, and A. Yu. Smirnov, Phys. Rev. D **58**, 096016 (1998); G. L. Fogli, E. Lisi, D. Montanino, and A. Palazzo, *ibid.* **62**, 013002 (2000).
[7] C. Athanassopoulos *et al.*, Phys. Rev. Lett. **75**, 2650 (1995); **77**, 3082 (1996); **81**, 1774 (1998); LSND Collaboration, R. L. Imlay, in *ICHEP 2000*, Proceedings of the 30th International Conference on High Energy Physics, Osaka, 2000, edited by C. S. Lim and T. Yamanaka (World Scientific, Singapore, 2001), p. 950.
[8] SNO Collaboration, Q. R. Ahmad *et al.*, Phys. Rev. Lett. **87**, 071301 (2001).
[9] G. L. Fogli, E. Lisi, D. Montanino, and A. Palazzo, Phys. Rev. D **64**, 093007 (2001); J. N. Bahcall, M. C. Gonzalez-Garcia, and C. Peña-Garay, J. High Energy Phys. **08**, 014 (2001); A. Bandyopadhyay, S. Choubey, S. Goswami, and K. Kar, Phys. Lett. B **519**, 83 (2001).
[10] V. Barger, P. Langacker, J. Leveille, and S. Pakvasa, Phys. Rev. Lett. **45**, 692 (1980); V. Barger, N. Deshpande, P. B. Pal, R. J. N. Phillips, and K. Whisnant, Phys. Rev. D **43**, 1759 (1991).
[11] X. Shi, D. N. Schramm, and B. D. Fields, Phys. Rev. D **48**, 2563 (1993); S. M. Bilenky and C. Giunti, Phys. Lett. B **320**, 323 (1994).
[12] D. O. Caldwell, *Perspectives in Neutrinos, Atomic Physics and Gravitation* (Editions Frontières, Gif-sur-Yvette, France, 1993), p. 187; D. O. Caldwell and R. N. Mohapatra, Phys. Rev. D **48**, 3259 (1993); J. T. Peltoniemi and J. W. F. Valle, Nucl. Phys. **B406**, 409 (1993); J. R. Primack, J. Holtzman, A. Klypin, and D. O. Caldwell, Phys. Rev. Lett. **74**, 2160 (1995); E. J. Chun, A. S. Joshipura, and A. Yu. Smirnov, Phys. Lett. B **357**, 608 (1995); J. J. Gomez-Cadenas and M. C. Gonzalez-Garcia, Z. Phys. C **71**, 443 (1996).
[13] S. M. Bilenky, C. Giunti, and W. Grimus, Eur. Phys. J. C **1**, 247 (1998).
[14] S. M. Bilenky, C. Giunti, C. W. Kim, and S. T. Petcov, Phys. Rev. D **54**, 4432 (1996); S. M. Bilenky, C. Giunti, and W. Grimus, *ibid.* **57**, 1920 (1998); **58**, 033001 (1998).
[15] E. Ma and P. Roy, Phys. Rev. D **52**, 4780 (1995); A. Yu. Smirnov and M. Tanimoto, *ibid.* **55**, 1665 (1997).
[16] S. Goswami, Phys. Rev. D **55**, 2931 (1997).
[17] N. Okada and O. Yasuda, Int. J. Mod. Phys. A **12**, 3669 (1997).
[18] V. Barger, T. J. Weiler, and K. Whisnant, Phys. Lett. B **427**, 97 (1998); V. Barger, S. Pakvasa, T. J. Weiler, and K. Whisnant, Phys. Rev. D **58**, 093016 (1998).
[19] V. Barger, Y.-B. Dai, K. Whisnant, and B.-L. Young, Phys. Rev. D **59**, 113010 (1999).
[20] Super-Kamiokande Collaboration, S. Fukuda *et al.*, Phys. Rev. Lett. **86**, 5656 (2001).
[21] Super-Kamiokande Collaboration, S. Fukuda *et al.* Phys. Rev. Lett. **85**, 3999 (2000).
[22] V. Barger, D. Marfatia, and K. Whisnant, Phys. Rev. Lett. **88**, 011302 (2002).
[23] M. C. Gonzalez-Garcia, M. Maltoni, and C. Peña-Garay, Phys. Rev. D **64**, 093001 (2001); hep-ph/0108073.
[24] M. Tanimoto, Phys. Rev. D **55**, 322 (1997); J. Arafune and J. Sato, *ibid.* **55**, 1653 (1997).
[25] J. Arafune, M. Koike, and J. Sato, Phys. Rev. D **56**, 3093 (1997); **60**, 119905(E) (1999).
[26] H. Minakata and H. Nunokawa, Phys. Lett. B **413**, 369 (1997); Phys. Rev. D **57**, 4403 (1998).
[27] M. Koike and J. Sato, Phys. Rev. D **61**, 073012 (2000); **62**, 079903(E) (2000).
[28] K. Dick, M. Freund, M. Lindner, and A. Romanino, Nucl. Phys. **B562**, 29 (1999).
[29] T. Ota and J. Sato, Phys. Rev. D **63**, 093004 (2001); T. Miura, E. Takasugi, Y. Kuno, and M. Yoshimura, *ibid.* **64**, 013002 (2001).
[30] L. Wolfenstein, Phys. Rev. D **17**, 2369 (1978); V. Barger, K. Whisnant, S. Pakvasa, and R. J. N. Phillips, *ibid.* **22**, 2718 (1980); P. Langacker, J. P. Leveille, and J. Sheiman, *ibid.* **27**, 1228 (1983); S. P. Mikheev and A. Yu. Smirnov, Sov. J. Nucl. Phys. **42**, 913 (1985).
[31] H. Minakata and H. Nunokawa, Phys. Lett. B **495**, 369 (2000); S. J. Parke and T. J. Weiler, *ibid.* **501**, 106 (2001); P. Lipari, Phys. Rev. D **64**, 033002 (2001); E. K. Akhmedov, Phys. Lett. B **503**, 133 (2001); O. Yasuda, *ibid.* **516**, 111 (2001).
[32] A. De Rújula, M. B. Gavela, and P. Hernández, Nucl. Phys. **B547**, 21 (1999); V. Barger, S. Geer, R. Raja, and K. Whisnant, Phys. Rev. D **62**, 073002 (2000); A. Cervera, A. Donini, M. B. Gavela, J. J. Gomez Cádenas, P. Hernández, O. Mena, and S. Rigolin, Nucl. Phys. **B579**, 17 (2000); **B593**, 731(E) (2001).
[33] V. Barger, S. Geer, R. Raja, and K. Whisnant, Phys. Rev. D **63**, 113011 (2001).
[34] S. M. Bilenky, C. Giunti, and W. Grimus, Phys. Rev. D **58**, 033001 (1998); A. Kalliomäki, J. Maalampi, and M. Tanimoto, Phys. Lett. B **469**, 179 (1999); A. Donini, M. B. Gavela, P. Hernández, and S. Rigolin, Nucl. Phys. **B574**, 23 (2000); Nucl. Instrum. Methods Phys. Res. A **451**, 58 (2000).
[35] T. Hattori, T. Hasuike, and S. Wakaizumi, Phys. Rev. D **62**, 033006 (2000).
[36] V. Barger, S. Geer, R. Raja, and K. Whisnant, Phys. Rev. D **63**, 033002 (2001).
[37] A. Donini and D. Meloni, Eur. Phys. J. C **22**, 179 (2001).
[38] Z. Maki, M. Nakagawa, and S. Sakata, Prog. Theor. Phys. **28**, 870 (1962).
[39] S. M. Bilenky and B. Pontecorvo, Phys. Rep. **41**, 225 (1978).
[40] V. Barger, B. Kayser, J. Learned, T. Weiler, and K. Whisnant, Phys. Lett. B **489**, 345 (2000); O. L. G. Peres and A. Yu. Smirnov, Nucl. Phys. **B599**, 3 (2001); W. Grimus and T. Schwetz, Eur. Phys. J. C **20**, 1 (2001).
[41] B. Achkar *et al.*, Nucl. Phys. **B434**, 503 (1995).
[42] M. Apollonio *et al.*, Phys. Lett. B **420**, 397 (1998); **466**, 415 (1999).
[43] CHORUS Collaboration, E. Eskut *et al.*, Phys. Lett. B **424**, 202 (1998); **434**, 205 (1998).
[44] NOMAD Collaboration, P. Astier *et al.*, Phys. Lett. B **453**, 169 (1999); **471**, 406 (2000); **483**, 387 (2000).
[45] MINOS Collaboration, P. Adamson *et al.*, NuMI-L-337, 1998.
[46] OPERA Collaboration, M. Guler *et al.* CERN-SPSC-2000-028, CERN-SPSC-P-318, LNGS-P25-00, 2000.
[47] JHF Neutrino Working Group, Y. Itow *et al.*, Letter of Intent, KEK report 2001-4, ICRR-report-477-2001-7, TRI-PP-01-05, hep-ex/0106019.